range requires a rather large exchange for a rare-earth system. This suggests finding an intermetallic compound rather than an insulator.

Cubic intermetallic compounds with singlet ground states, especially the rare-earth group V compounds, are available. Indeed, the transition from Van Vleck paramagnetism to antiferromagnetism with increasing exchange (i.e., Tb content) has been observed[18] for $Tb_xY_{1-x}Sb$. However, much of the behavior becomes more complex (particularly the question of a first-order magnetic transition) when the excited state is a triplet.

[18] B. R. Cooper and O. Vogt (unpublished). Some of the results for $Tb_xY_{1-x}Sb$ are quoted in B. R. Cooper, J. Appl. Phys. **40**, 1344 (1969).

It would be very interesting, whether in a singlet-singlet or a singlet-triplet system, to study the specific heat in a number of compounds where the ratio of ordering temperature to crystal-field splitting varied. This would change the relative location and integrated area under the peaks, such as shown in Fig. 11. If alloying did not broaden out the peak at the ordering temperature too greatly, use of an alloy system such as $Tb_xY_{1-x}Sb$ to study such effects could be quite interesting.

ACKNOWLEDGMENTS

We have enjoyed interesting discussions with Professor W. Wolf. We are grateful to Miss E. Kreiger for aid with the numerical calculations.

PHYSICAL REVIEW VOLUME 185, NUMBER 2 10 SEPTEMBER 1969

Antiferromagnetic Phase Diagram and Magnetic Band Gap Shift of $NaCrS_2$

K. W. BLAZEY AND H. ROHRER
IBM Zurich Research Laboratory, 8803 Rüschlikon-ZH, Switzerland
(Received 27 March 1969)

The magnetization and differential susceptibility of the layer-structured compound $NaCrS_2$ have been measured parallel and perpendicular to the c axis in pulsed magnetic fields up to 200 kOe as a function of temperature. Antiferromagnetic ordering was observed below 18°K. For fields applied parallel to the Cr layers, a spin-flop-type transition was observed at 20 kOe and a transition to the paramagnetic phase observed at higher fields. The temperature dependence of the latter transition is found to vary as the sublattice magnetization computed from the parallel susceptibility. The in-plane and out-of-plane anisotropies are due to intraplane dipolar interactions and are of comparable magnitude, ~3 kOe. The optical absorption spectrum has been measured in the range 1–2.4 eV where the charge-transfer band gap occurs. Measurements as a function of temperature show that the *d-d* crystal-field transitions observed between 1.5 and 1.9 eV, are only slightly affected on passing through the Néel temperature, whereas the band gap shows an anomalously large blue-shift. This is thought to be evidence against the recent theory that these magnetic shifts are due to deformation potentials and magnetoelastic coupling. An alternative explanation is presented in which the band gap shift is due to the different exchange interactions in the ground and excited states.

INTRODUCTION

THE magnetic phase diagram of antiferromagnetic materials has been the subject of careful study recently, both theoretically[1,2] and experimentally. Most of the experimental studies have been restricted to the antiferromagnetic spin-flop phase transition[3] and only for materials with low Néel temperatures, such as $MnCl_2 \cdot 4\ H_2O$ [4] and $GdAlO_3$,[5] has the complete phase diagram been determined.

[1] J. Feder and E. Pytte, Phys. Rev. **168**, 640 (1968).
[2] C. J. Gorter and T. van Peski-Tinbergen, Physica **22**, 273 (1956); F. B. Anderson and H. B. Callen, Phys. Rev. **136**, 1068 (1964); H. Rohrer and H. Thomas, J. Appl. Phys. **40**, 1025 (1969).
[3] J. H. Danicar and P. R. Elliston, Phys. Letters **25A**, 720 (1967).
[4] J. E. Rives, Phys. Rev. **162**, 491 (1967).
[5] K. W. Blazey and H. Rohrer, Phys. Rev. **173**, 574 (1968); K. W. Blazey, H. Rohrer, and R. Webster, Conference on High Magnetic Fields and Their Application, University of Nottingham, England, 1969 (unpublished).

The temperature variation of the band gap of magnetic semiconductors has also been given considerable attention. The two groups of materials which have been most extensively studied are the europium chalcogenides[6] and the chromium-containing spinels.[7] On cooling these different crystals below their ordering temperatures, both red- and blue-shifts of the optical band gap have been observed. This magnetic shift in the europium chalcogenides has been ascribed to an exchange splitting of the excited state[8] and has also been related to the sample magnetization.[9] More re-

[6] G. Busch, P. Junod, and P. Wachter, Phys. Letters **12**, 822 (1965); B. E. Argyle, J. C. Suits, and M. J. Freiser, Phys. Rev. Letters **15**, 822 (1965).
[7] G. Harbeke and H. Pinch, Phys. Rev. Letters **17**, 1090 (1966).
[8] F. Rys, J. S. Helman, and W. Baltensperger, Physik Kondensierten Materie **6**, 105 (1967).
[9] G. Busch and P. Wachter, Physik Kondensierten Materie **5**, 232 (1966).

cently, such shifts have been attributed to deformation potentials and magnetoelastic coupling.[10]

Here we report measurements of the magnetic phase diagram, the magnetic shift of the optical band gap, and the sublattice magnetization derived from the parallel susceptibility for the compound $NaCrS_2$. The results show that in this low anisotropy antiferromagnet the spin-flop–paramagnet phase boundary follows closely the sublattice magnetization as predicted by molecular field theory. The optical band gap, however, does not vary as the sublattice magnetization but more as a spin-spin correlation function as predicted by the theories of Refs. 8 and 10. Furthermore, the different temperature dependences of the optical band gap and the crystal-field transitions of the Cr^{3+} ion provide evidence against the band gap shift being associated with deformation potentials and magnetoelastic coupling.

The crystal structure of $NaCrS_2$ was reported to be a layer structure as shown in Fig. 1 by Rüdorff and Stegemann,[11] this is also apparent from the crystals which are micalike shiny metallic-looking platelets. The crystals were prepared by the method described by Rüdorff and Stegemann. The crystals obtained were sheets of about 0.1 mm thickness consisting of little platelets with a common well-defined c axis perpendicular to the layer, but are polycrystalline within the layer plane.

Some magnetic properties of $NaCrS_2$ have been previously reported by Bongers *et al.*,[12] who report a transition to antiferromagnetism below 19°K. The same group also observed the spin-flop transition in their magnetization curves when the magnetic field was applied parallel to the platelets.

The first section of this paper will be devoted to the magnetic properties of $NaCrS_2$ derived from magnetization and differential susceptibility measurements. The optical absorption spectrum will be discussed in the second section.

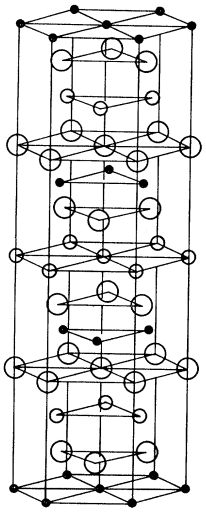

FIG. 1. Crystal structure of $NaCrS_2$ [after Rudroff and Stegemann, Z. Anorg. Allgem. Chem. **251**, 376 (1943)]. Sulfur ○; sodium ○; chromium ●.

MAGNETIC MEASUREMENTS

Experiment

The thin crystal platelets were cut to make composite samples of cylindrical form with the c axis parallel or perpendicular to the cylinder axis. The samples were about 1mm diam and 7 mm long so that demagnetizing effects for fields applied along the cylinder axis were small. In this way, one obtains the magnetization for fields perpendicular to the layer plane but only an average (averaged over the layer plane) magnetization for fields in the layer.

The samples were mounted in Perspex tubes that fitted into a pickup coil and heater arrangement inside a pulsed magnetic field coil. Not only were the magnetization M and applied field H obtained by integrating their time derivatives, but the differential susceptibility dM/dH was also determined by dividing these two time derivatives as described earlier.[5] The magnetization measurement was calibrated against pure iron and the magnetic field was calibrated with the calculated coil factors.

Results

In Fig. 2, the inverse molar susceptibility is plotted against temperature. At temperatures above 140°K, $1/\chi_M$ has been found to vary linearly with temperature.[12] The straight line drawn through the point at 140°K and room temperature yields the expected Curie

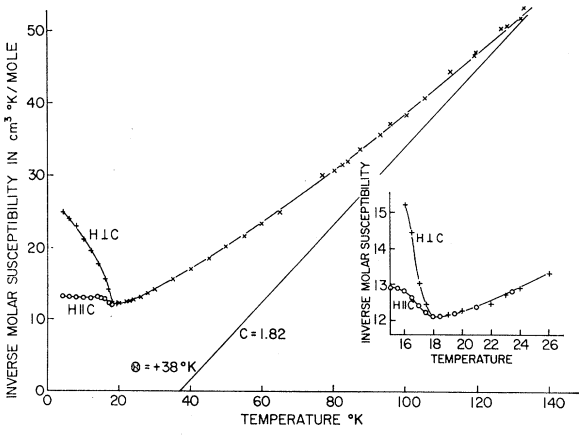

FIG. 2. Inverse molar susceptibility as a function of temperature. The susceptibility for $H \perp c$ is the parallel susceptibility averaged over the layer plane, $\bar{\chi}_{\perp}$.

[10] Earl Callen, Phys. Rev. Letters **20**, 1045 (1968).
[11] W. Rüdorff and K. Stegemann, Z. Anors. Allgem. Chem. **251**, 376 (1943).
[12] P. F. Bongers, C. F. van Bruggen, J. Koopstra, W. P. F. A. M. Omloo, G. A. Wiegers, and F. Jellinek, J. Phys. Chem. Solids **29**, 977 (1968).

constant for Cr^{3+} to within the experimental error, and gives a Curie-Weiss Θ_p of 38°K, indicating that ferromagnetic exchange interactions are dominant.

Below 140°K, a distinct curvature away from the Curie-Weiss law is observed as would be expected for a two-dimensional array of magnetic ions.[13] This is consistent with the $NaCrS_2$ crystal structure which shows layers of Cr^{3+} ions well separated from each other by one sodium and two sulfur layers. Another consequence of this layered crystal structure is that the exchange interaction between Cr^{3+} ions within a layer should be much stronger than the interlayer exchange interaction. Because the Curie-Weiss Θ_p is positive, this stronger intralayer exchange is thought to be ferromagnetic. At 18°K, the inverse susceptibility shows a minimum typical of a transition to antiferromagnetic order. Below the transition temperature, the susceptibility $\chi_\perp$ measured perpendicular to the Cr^{3+} layers (parallel to the c axis) is nearly temperature-independent, whereas with $\bar{\chi}_{\parallel}$, the susceptibility measured parallel to the layer plane decreases. This shows that the sublattice magnetizations in the ordered state lie within the planes and each layer plane may be ferromagnetically aligned. The fact, that at low temperatures $\bar{\chi}_{\parallel}$ for fields in the layer plane decreases to only half its value at the transition temperature, has been interpreted as being due to a helical arrangement of the ferromagnetic layers with a turn angle close to π.[12] However, because of the crystalline nature of the samples, the measured susceptibility $\bar{\chi}_{\parallel}$ is an averaged value over the layer plane. A simple antiferromagnetic alignment of the ferromagnetic layers with an easy axis in the layer plane would also give the same result, since in this case the averaged susceptibility $\bar{\chi}_{\parallel}$ is given by[14]

$$\bar{\chi}_{\parallel}=\tfrac{1}{2}(\chi_{\parallel}+\chi_{\perp}).$$

More evidence in favor of this simple antiferromagnetic model is presented later on.

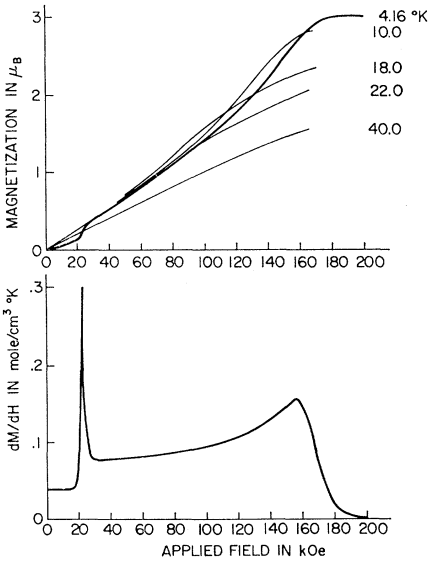

FIG. 3. (a) Magnetization curves for various temperatures; (b) differential susceptibility versus applied field at $T=4.16$°K.

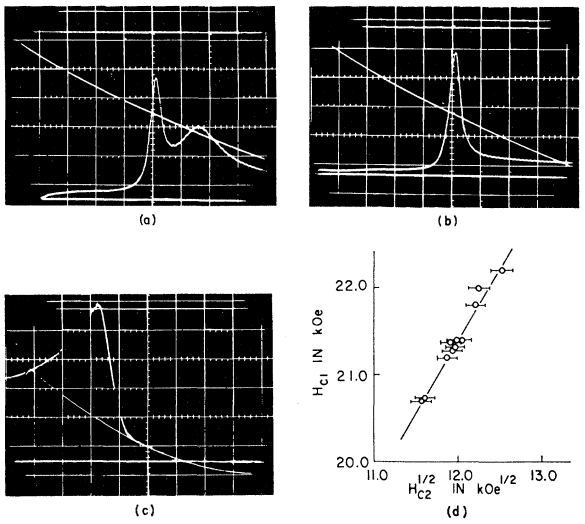

FIG. 4. Phase transitions. (a)–(c) show the differential susceptibility at the phase transitions as a function of applied field. The difference between the two lines starting from the upper left corner gives the magnetic field [7.35 kOe per scale div. in (a) and (b) and 36.75 kOe per scale div. in (c)], and that between the two lines starting from the lower left corner gives the differential susceptibility, in arbitrary units. The antiflop transition for an unstrained sample is shown in (a), that for a strained sample (same sample as in Fig. 3) is shown in (b). The narrow peak moves from 20.7 to 22.2 kOe, while the wide peak disappears. The flop-para transition of an unstrained sample is shown in (c). Figure 4 (d) gives the relation between the antiflop field H_{c1} and the flop-para field H_{c2} for differential strained samples; the error in H_{c1} is about 0.1 kOe.

In Fig. 3(a), the magnetization with the applied field in the layer plane is shown as a function of field and temperature. At around 21 kOe, the magnetization jumps to its value for fields applied perpendicular to the layer plane. Above this spin-flop-type transition the magnetization first increases linearly with the applied field. Before leveling off to the saturation value of $3\mu_B$ per atom, the magnetization increases rapidly. The field for maximal slope of the high-field M-H curves locates the second-order transition to the paramagnetic state. For fields applied perpendicular to the layer plane, the magnetization curve is identical to that of the parallel case except of course no spin-flop-type transition is observed.

The phase transitions can be located better if dM/dH is considered rather than M as illustrated in Fig. 3(b), where dM/dH is plotted against applied field for 4.16°K. The high peak in dM/dH at around 21 kOe marks the

[13] N. D. Marvin and H. Wagner, Phys. Rev. Letters **17**, 1133 (1966).

[14] Since the anisotropy is small compared to the exchange, the perpendicular susceptibility for fields in the layer is equal to $\chi_\perp$, the susceptibility for fields perpendicular to the layer.

spin-flop transition at H_{c1} and the sharp drop at high fields locates the transition to the paramagnetic state at H_{c2}. In molecular field theory, the differential susceptibility dM/dH is independent of field and temperature between the two transitions and is equal to the perpendicular susceptibility. The deviations found experimentally are attributed to spin-wave effects such as zero-point deviations[15] and critical fluctuations[1] which make the susceptibility singular at the flop-para transition. The factor of 2 between the low-field susceptibility just above H_{c1}, and the susceptibility just below H_{c2} demonstrates the enhanced importance of the zero-point deviations in the case of a nearly two-dimensional magnetic structure as opposed to a three-dimensional structure.[15,16] A more detailed treatment of this effect will be given in a separate paper.

The transitions are sensitive to mechanical strain. In the case of the spin-flop field H_{c1}, a narrow high peak followed by a wide small peak is found [Fig. 4(a)] in an unstrained (no external stress) sample. With increasing strain the wide peak gets smaller and eventually disappears [Fig. 4(b)], whereas, the narrow peak gets higher and also moves to a slightly higher field. Experimentally, the external stress comes about because the stack of platelets is enclosed in Plexiglas tubes and various strains are produced by packing the samples tightly. Because the strains so obtained are not well defined (neither in magnitude nor in direction) no detailed statements can be made on this pressure effect. We can, however, relate the changes of the different parameters. Simultaneously with the increase of the field of the narrow spin-flop peak, the flop-para field H_{c2} and the Néel temperature T_N increase. One finds that $2\Delta H_{c1}/H_{c1} \approx \Delta H_{c2}/H_{c2}$ [Fig. 4(d)]. But $H_{c1} \propto (H_{an}H_{ex})^{1/2}$ and $H_{c2} \propto H_{ex}$,[5] where H_{an} is the anisotropy field and H_{ex} the exchange field. Therefore, mechanical stress mainly affects the interlayer isotropic exchange and leaves the anisotropy field nearly unchanged. Furthermore, the measured relative change of T_N is only slightly less than that of H_{c2}. Because in $NaCrS_2$ the dominant part of T_N is the intralayer exchange, the intralayer isotropic exchange is similarly affected by the mechanical strain as the interlayer exchange. We conclude then that mechanical stress strongly affects the isotropic exchange interactions and only weakly affects the anisotropy.

In Fig. 5 is plotted the phase diagram for two unstrained samples with the field applied perpendicular and parallel to the layer plane. The antiflop boundary is nearly temperature-independent, showing a very shallow minimum at 12°K. It meets the transition curve to the paramagnetic region in a triple point[17] as found in $GdAlO_3$.[5] The transition to the paramagnetic state has been measured by sweeping the field at constant temperature [Fig. 4(c)] for temperatures below 17°K (vertical error lines), and for temperatures above 17°K the magnetization was measured at constant field for varying temperatures (horizontal error lines). In the case of strained samples showing a single peak at the spin-flop transition, two maxima in the magnetization as a function of temperature were observed for fields below 22 kOe. This branching of the outer phase boundary below the triple point is not understood.

The low-temperature values of $H_{c1}=21$ kOe and $H_{c2}=138$ kOe may be used to determine the anisotropy field by insertion into $H_a=H_{c1}^2/H_{c2}$, which yields $H_a=3.2$ kOe. EPR experiments on Cr-doped $NaInS_2$ have shown[18] that the crystal-field anisotropy $2D$ is small $\sim$0.4 kOe, which in addition would align the Cr spins parallel to the c axis. Crystal-field anisotropy may, therefore, safely be neglected in the following, as would be expected for a crystal-field S-state ion. Similarly, the contribution of anisotropic exchange to the anisotropy field is expected to be small and the anisotropy is therefore attributed to dipolar anisotropy. For a ferromagnetically aligned layer, dipolar interactions keep the spins in the layer plane and give the necessary out-of-plane anisotropy. An additional in-plane dipolar anisotropy or antiferromagnetic exchange between second nearest planes (in the case of helical spin structure) prevents the spins from freely turning in the plane. The inplane dipolar anisotropy might be produced by a distortion of the hexagonal pattern of the layer. The existence of such a distortion is also indicated by NMR experiments[19] which show four different Cr sites to exist below the ordering temperature. In the case of a helical structure, the experimentally found ratio of the two critical fields at low temperatures $H_{c2}/H_{c1} \sim 7$ gives

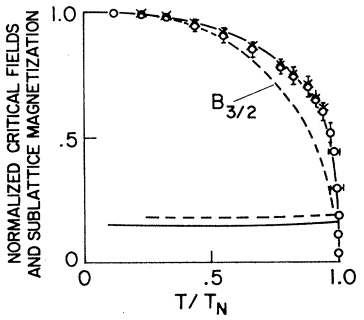

FIG. 5. Magnetic phase diagram of an unstrained sample. The critical fields are normalized to $H_{c2}(\perp, 0°K)=1$, the sublattice magnetization to $\sigma(0°K)=1$. The solid and broken horizontal lines give the measured fields of the narrow and wide peak, respectively, at the antiflop transition. The circles and crosses are the measured flop-para fields with the magnetic field parallel and perpendicular to the layer plane, respectively. The solid line represents the sublattice magnetization calculated from the parallel susceptibility. $B_{3/2}$ represents the Brillouin function for $S=\frac{3}{2}$.

[15] I. S. Jacobs and S. D. Silverstein, Phys. Rev. Letters **13**, 272 (1964).
[16] P. W. Anderson, Phys. Rev. **86**, 694 (1952).
[17] H. Rohrer and H. Thomas (unpublished).
[18] K. A. Müller and W. Berlinger, Phys. Rev. **175**, 503 (1968). In this paper $\frac{1}{2}H_a$ is compared with D.
[19] W. G. Moulton (private communication).

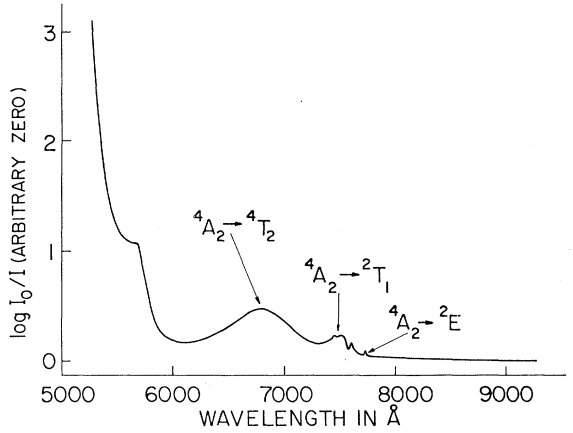

FIG. 6. The axial absorption spectrum of $NaCrS_2$ taken at 5°K.

a turn angle of 148°.[20] This implies a ratio of the perpendicular to the parallel susceptibility at low temperatures of 1.57 instead of 2 as experimentally found. We therefore conclude that $NaCrS_2$ orders in a simple antiferromagnetic structure with in-plane and out-of-plane anisotropy rather than in a helical structure. This is further supported by preliminary measurements on more perfect crystals where $\chi_\perp/\bar{\chi}_{||}$ varies between 2.5 and 1.5 for crystals cut parallel to and bisecting the hexagonal axes, respectively.

Hornreich and Strickmann[21] have shown that the relation between the parallel susceptibility $\chi_{||}$ and the sublattice magnetization σ in a two-sublattice antiferromagnet derived within the molecular field approximation should hold even if $\chi_{||}$ and σ each deviated substantially from their molecular field values. Because in the molecular field approximation the flop-para critical field in the hard direction, $H_{c2}(\perp)$, is proportional to the zero-field sublattice magnetization,[17] it is interesting to test the hypothesis of Hornreich and Strickmann also for the relation between $\chi_{||}$ and $H_{c2}(\perp)$. From the measured averaged parallel susceptibility and the perpendicular susceptibility, one obtains the parallel susceptibility $\chi_{||}=2\bar{\chi}_{||}-\chi_\perp$. This $\chi_{||}$ has been used to compute the temperature dependence of the sublattice magnetization which is shown in Fig. 5. The good agreement found between σ computed from $\chi_{||}$ and that derived from $H_{c2}(\perp)$ is remarkable in two respects. First, the Hamiltonian used by Hornreich and Strickmann does not allow for zero-point deviations. As shown above, such deviations might substantially influence the susceptibility, but leave the flop-para field H_{c2} unaffected. Second, the parallel susceptibility used here was derived from an averaged susceptibility and the perpendicular susceptibility, which according to Hornreich and Strickmann[21] leads to additional complications.

[20] T. Nagamiya, K. Nagata, and Y. Kitano, Progr. Theoret. Phys. (Kyoto) **27**, 1253 (1962).
[21] R. Hornreich and S. Strickmann, Phys. Rev. **159**, 408 (1967).

The critical field $H_{c2}(0°K)$ together with the paramagnetic Curie-Weiss temperature Θ_p are best suited to determine the intralayer and interlayer exchange constants per atom, J_0 and J_1, respectively. In the molecular field approximation, the interaction constants can be calculated in principle from any two of the measured values of Θ_p, T_N, $\chi_\perp$, or H_{c2}. However, effects like short-range order and zero-point deviations, which are not included in the molecular field approximation, make the molecular field expressions for T_N and $\chi_\perp$ no longer adequate in this case. Short-range order gives rise to a curved susceptibility graph and thus seriously affects both T_N and $\chi_\perp(T_N)$. Below T_N, the zero-point deviations cause a reduction in $\chi_\perp$. Both $H_{c2}(0°K)$ and Θ_p, however, are not affected by short-range order or zero-point deviations and may therefore be used to

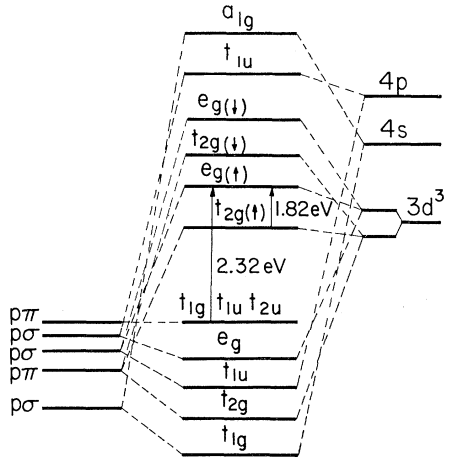

FIG. 7. Schematic molecular orbital scheme of the CrS_6 octahedron. The p orbitals originate from the sulfur atoms and the $3d$, $4s$, and $4p$ orbitals from the chromium atoms. The arrows indicate the $^4A_2 \rightarrow {}^4T_2$ transition at 1.82 eV and the optical band gap at 2.32 eV. This level scheme is a single-electron model and thus is misleading in giving the energies of the final states which have their energies determined by many-body effects. Thus, although both transitions promote an electron into an $e_g(\uparrow)$ orbital, the final states will have different energies due to the different electron concentration on the chromium ions. This energy difference is not shown in this diagram.

determine J_0 and J_1. From

$$H_{c2}=-2J_1S/g\mu_B \qquad =138 \text{ kOe},$$
$$\Theta_p=\tfrac{1}{3}S(S+1)(J_0+J_1)=38°\text{K},$$

one obtains $J_0/k=36.2°$K and $J_1/k=-6.2°$K.

Because the samples used are not single crystals in the layer plane we cannot make detailed statements about the different anisotropies. We can, however, argue qualitatively that the in-plane and out-of-plane anisotropies are of comparable magnitude and that both are of the order of 3 kOe. The anisotropies are due to intralayer dipole interactions and therefore add to or subtract from the critical field H_{c2}, depending on whether the field is applied parallel or perpendicular to the corresponding anisotropy field.[5] Because H_{c2} for

fields applied in the layer and perpendicular to the layer is nearly the same (Fig. 5), the corresponding anisotropies (in-plane and out-of-plane anisotropy, respectively) have to be of comparable magnitude.

Furthermore, the hard axis is the c axis as can be seen from the following: If the hard axis is in the layer plane, the measured spin-flop field is an average of spin-flop fields given by the critical hyperbola.[22] In the case of a narrow hyperbola (nearly equal anisotropies), only few crystallites would contribute to the spin flop and the increase of the magnetization at the spin-flop transition would be very small. In the case of a wide hyperbola (substantially different anisotropies) the measured spin-flop transition would be smeared out. Because neither of these cases is observed, we conclude that the hard direction is along the c axis.

OPTICAL MEASUREMENTS

The optical absorption spectrum of thin $NaCrS_2$ platelets has been measured as a function of temperature, above and below the ordering temperature. Light from a $\frac{1}{2}$-m Ebert monochromator was focused at the sample mounted in the cold finger of a liquid-helium cryostat. The transmitted light was detected with a S-1 response photomultiplier, cooled in dry ice and alcohol, and a lock-in amplifier.

The axial absorption spectrum of the thinnest sample used, which was about 2 μ thick, is shown in Fig. 6. The principal features are a charge-transfer band gap near 5300 Å with further band and sharp line absorptions at longer wavelengths. Similar spectra have been reported for Cr_2O_3[23] and the chromium trihalides.[24] The molecular orbital energy level scheme envisaged here in $NaCrS_2$ is similar to that given in Ref. 24 for $CrBr_3$ and is shown here in Fig. 7. It is not thought that the sodium orbitals play an important role in the optical absorption spectrum as they lie much higher in energy than the chromium and sulfur orbitals.

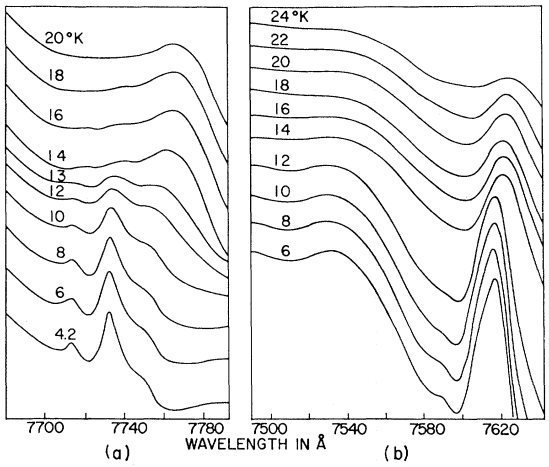

FIG. 8. The temperature variation of the axial absorption spectrum of $NaCrS_2$ in the region of the $^4A_2 \rightarrow {}^2E$ (a) and $^4A_2 \rightarrow {}^2T_1$ (b) transition is $NaCrS_2$.

The weak band absorptions between 6000 and 8000 Å are characteristic of the d-d crystal-field transitions[25] of Cr^{3+} and are labelled accordingly in Fig. 6. The lowest energy absorption is the $^4A_2 \rightarrow {}^2E$ transition which is the "R-line" fluorescent transition in ruby. Despite there being little other absorption in this region, at low temperatures, apart from this transition, no fluorescence was observed. The temperature variation of the absorption in this region is shown in more detail in Fig. 8(a). At the lowest temperature, only two absorption lines are seen clearly. On warming, these lose their intensity and another line at longer wavelengths, presumably a transition from the next highest level in the ground state, grows in intensity and moves to lower energies. The separation of the two low-temperature lines does not decrease markedly with increasing temperature as would be expected for an exchange splitting. But since most of the decrease should occur near T_N, where the lines are no longer observed, this result is not unexpected.

It has been shown previously[26] that the molecular field approximation is not applicable to this transition in Cr_2O_3. More recently,[27] the separation of the two lines seen in the axial spectrum of Cr_2O_3 has been interpreted as a Davydov splitting of the ^2E level due to the transfer of excitation via the intrasublattice exchange. This is possible only with more than two magnetic ions per unit cell. This is also the case in $NaCrS_2$ where NMR[19] data show that there are four magnetic sites per unit cell in the ordered state. Following the analysis of Ref. 27, the Davydov splitting is estimated to be 38 cm^{-1} from the intrasublattice exchange obtained from the magnetic data. The observed splitting of 31 cm^{-1} is in reasonable agreement with this estimate.

The absorption in the region labelled $^4A_2 \rightarrow {}^2T_1$ in Fig. 6 may also contain phonon sidebands of the ^2E level. The sharp structure in this region shown in Fig. 8(b) is affected less than the $^4A_2 \rightarrow {}^2E$ transitions on passing through the ordering temperature. Here again, there is a change of intensity of the main absorption line, but since it is also present at the Néel temperature the line shift may be determined. On cooling into the ordered state, the line shifts to higher energy by 18 cm^{-1}, which is about half that predicted from the known internal field and may be explained by a larger exchange interaction in the excited state.

Both the $^4A_2 \rightarrow {}^4T_2$ and the band gap transitions have been observed in the diffuse reflection spectra.[28] The

[22] J. Ubbink, Physica **19**, 9 (1953); T. Nagamiya, Progr. Theoret. Phys. (Kyoto) **11**, 309 (1954).
[23] D. S. McClure, J. Chem. Phys. **38**, 2289 (1963).
[24] J. F. Dillon, Jr., H. Kamimura, and J. P. Remeika, J. Appl. Phys. **34**, 1240 (1963).
[25] Y. Tanabe and S. Sugano, J. Phys. Soc. Japan **9**, 766 (1954).
[26] J. P. van der Zeil, Phys. Rev. **161**, 483 (1967).
[27] J. W. Allen, R. M. Macfarlane, and R. L. White, Phys. Rev. (to be published).
[28] A. L. Companion and M. Mackin, J. Chem. Phys. **42**, 4219 (1965).

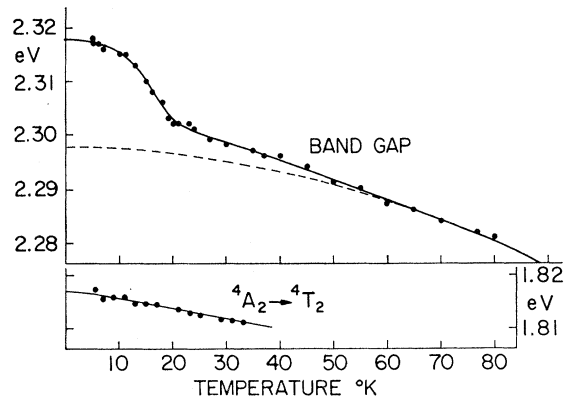

FIG. 9. The temperature variation of the $^4A_2 \rightarrow {}^4T_2$ transition and optical band gap of $NaCrS_2$. The broken line is the extrapolation of the phonon quadratic temperature dependence.

temperature variation of these transitions has been measured and is shown in Fig. 9. The band gap is arbitrarily defined at $\log I_0/I = 2$ above the absorption level at wavelengths near 9000 Å, where no temperature-dependent absorption was observed. There is no observable change in the temperature variation of the $^4A_2 \rightarrow {}^4T_2$ transition, and therefore $10Dq$, on cooling below the Néel temperature. This may be due to the large linewidth and uncertainty in defining the peak of the absorption. The band gap, however, shows a definite shift towards higher energies on cooling below 20°K. The total shift is 165 cm^{-1}, an order of magnitude larger than that observed for the sharp d-d transitions of the Cr^{3+} ion shown in Fig. 8.

The temperature variation of the band gap was found to be nearly linear from room temperature down to 200°K. Between 60 and 200°K the variation showed a square-law dependence as found in other semiconductors[29] of the form

$$E_g = E_0 - \alpha T^2,$$

where $E_0 = 2.298$ eV, $\alpha = 2.78 \times 10^{-6}$ eV/°K,^{2} and T is the temperature. Extrapolation of this square law to $T = 0$°K is shown in Fig. 9 and clearly reveals the effect of the magnetic ordering on the optical band gap at low temperatures.

There are two allowed transitions in the molecular orbital scheme shown in Fig. 7 for the CrS_6 octahedron that could be attributed to the optical band gap. In this orbital scheme all the orbitals are full, up to and including the $t_{2g}(\uparrow)$ orbitals, and those above the $t_{2g}(\uparrow)$ orbitals are empty. The allowed transitions are those from the sulfur nonbonding p orbitals to the $e_g(\uparrow)$ Cr^{3+} orbitals and those from the $t_{2g}(\uparrow)$ Cr^{3+} orbitals to the t_{1u} $Cr^{3+}4p$ orbitals. The latter $3d-4p$ transition is not observed in large band gap materials containing Cr^{3+} such as Al_2O_3 [30] and is therefore thought to be at energies greater than 4 eV. Because this transition would be expected to lie at about the same energy here, the optical band gap of $NaCrS_2$ is attributed to the sulfur $p\pi$-chromium $e_g(\uparrow)$ charge-transfer transition. The optical band gap of transition-metal salts has been assigned previously to this anion-cation charge transfer.[24,31]

Anomalously large shifts of the optical band gap in magnetic crystals as shown in Fig. 9 have recently been explained in terms of deformation potentials and magnetoelastic coupling. This explanation predicts a shift of the band gap dependent upon the sign and magnitude of the deformation potential.[10] Thus, both blue- and red-shifts are predicted. This is in contrast with the exchange model due to Rys *et al.*,[8] which predicts a blue-shift only if the initial state of the optical transition is on the magnetic ion, which is not thought to be the case here.

The magnetoelastic coupling model would require the deformation potential for the (S $p\pi$) $\rightarrow$ (Cr e_g) transition to be much larger than that for the $t_{2g}-e_g$ crystal-field transition. This is because the shifts of the d-d transitions are at least an order of magnitude smaller than the band gap shifts, and then of the size expected of the molecular field. The relative sizes of the deformation potentials are seen in the effect of hydrostatic pressure on the optical properties. Experiment shows that $10D_q$ is quite sensitive to hydrostatic pressure and changes as much as the band gaps of semiconductors like ZnS.[32] Furthermore, the temperature shifts observed above the ordering temperature which are due to deformation-potential electron-phonon coupling show only a difference of a factor 3 which would easily be observable in the magnetic region.

More recently, a measurement of the exchange striction in the chromium spinels has shown that a deformation potential of 100 eV would be required to explain the observed shift of optical band gap. This is larger than could reasonably be expected.[33]

It seems that an exchange model would be more appropriate here in explaining the anomalously large band gap shift that $NaCrS_2$ exhibits on passing through its Néel temperature. In particular, the following variation of the model used by Rys *et al.*[8] has been proposed by Freeman.[34] The sulfur $p\pi$-orbital initial state of the band gap transition is one where at the same time three 3-d electrons are on the Cr^{3+} ions which, in the ordered state, produce a net exchange field because of the ferromagnetic intralayer and antiferromagnetic interlayer-exchange interactions. On passing through the ordering temperature, the effect of this exchange field will be to split this initial state. The electron making the optical transition will have its spin parallel to the Cr^{3+} spin

[29] G. D. Mahan, J. Phys. Chem. Solids **26**, 751 (1965).
[30] D. S. McClure, in *Solid State Physics*, edited by F. Seitz and D. Turnbull (Academic Press Inc., New York, 1959), Vol. 9, p. 448.
[31] C. K. Jorgensen, Mol. Phys. **2**, 309 (1959).
[32] H. G. Drickamer, in *Solid State Physics*, edited by F. Seitz and D. Turnbull (Academic Press Inc., New York, 1965), Vol. 17, p. 1.
[33] G. W. Martin, A. T. Kellogg, R. L. White, R. M. White, and H. Pinch, J. Appl. Phys. **40**, 1015 (1969).
[34] A. Freeman (private communication).

and is therefore from the lower-exchange split-sulfur $p\pi$ orbital. This exchange splitting of the sulfur orbitals has recently been used by Goodenough[35] to explain the band gap shifts observed in the chromium thiospinels. The final state of the band gap transition is one with four electrons in the chromium d shell, three in the $t_{2g}(\uparrow)$ orbitals, and one in the $e_g(\uparrow)$ orbitals, and a hole in the sulfur p orbitals. This electron configuration will have a different exchange interaction with the neighboring Cr^{3+} ions. The effect of the extra hole will be to give an extra antiferromagnetic component to the ferromagnetic intralayer-exchange interaction. This antiferromagnetic component would raise the final state with respect to the initial state and thus would cause the observed blue-shift of the band gap. If the band gap transition were into a conduction band, then an extra ferromagnetic exchange contribution would arise and the observed shift would depend on the relative sizes of the extra exchange contributions. A dominant ferromagnetic exchange would cause a lowering of the final state and give a red-shift of the band gap.

The magnetic component of the optical band gap shift in such a model would depend on the magnetic energy whose temperature variation is given by the spin-correlation function. In Fig. 10, the normalized magnetic band gap shift is compared with the spin-correlation function and the sublattice magnetization. It is seen that the agreement with the spin-correlation function is much better than with the sublattice magnetization. This is to be expected since within the molecular field approximation the sublattice magnetization goes to zero at the ordering temperature, whereas, the correlation function includes short-range-order effects which are clearly seen in the band gap shift above the ordering temperature.

CONCLUSION

The antiferromagnetic phase diagram of $NaCrS_2$ has been measured and the flop-para phase boundary has been found to vary as the sublattice magnetization calculated from the parallel susceptibility. The molecular field parameters have been determined from the low-temperature flop-para critical field H_{c2} and the Curie-Weiss Θ_p in preference to the other measured quantities which are strongly affected by zero-point deviations.

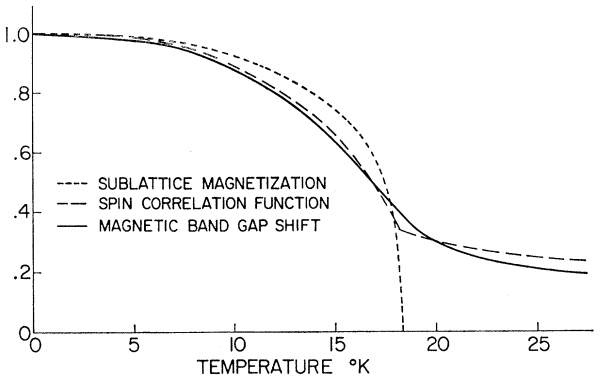

FIG. 10. Comparison of the normalized magnetic component of the optical band gap shift with the spin correlation function and the normalized sublattice magnetization.

The temperature variation of the optical-absorption spectrum, on cooling through the transition temperature, shows that the d-d crystal-field transitions of the Cr^{3+} ion are split or shifted by amounts not much different to that expected from the known internal fields. This is in contrast to the band gap which shifts by a larger energy which is thought to have its basis in many-body effects involving the band gap exciton. The temperature variation of the band gap has been found to follow the spin-correlation function rather than the sublattice magnetization.

ACKNOWLEDGMENTS

We should like to acknowledge stimulating discussions with A. Freeman, H. Thomas, G. Harbeke, K. A. Müller, E. Pytte, C. Schueler, E. Šimánek, and P. Wolf. We should also like to thank W. Moulton for communicating his results prior to publication. The crystal preparation by R. Meili and H. Scheel and the technical assistance of C. Gerber and R. Wey are gratefully acknowledged.

[35] J. B. Goodenough, J. Phys. Chem. Solids **30**, 261 (1969).

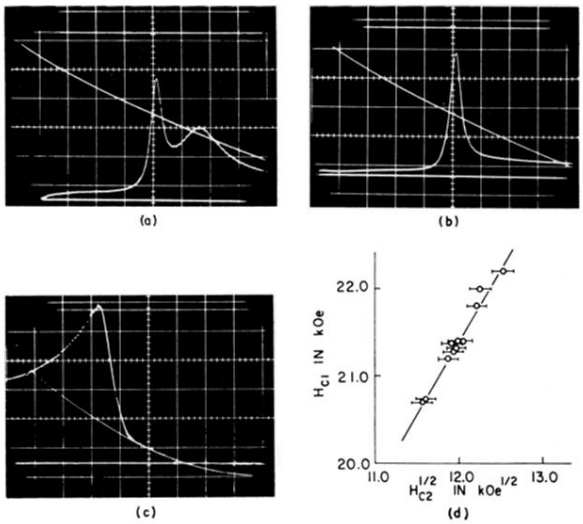

FIG. 4. Phase transitions. (a)–(c) show the differential susceptibility at the phase transitions as a function of applied field. The difference between the two lines starting from the upper left corner gives the magnetic field [7.35 kOe per scale div. in (a) and (b) and 36.75 kOe per scale div. in (c)], and that between the two lines starting from the lower left corner gives the differential susceptibility, in arbitrary units. The antiflop transition for an unstrained sample is shown in (a), that for a strained sample (same sample as in Fig. 3) is shown in (b). The narrow peak moves from 20.7 to 22.2 kOe, while the wide peak disappears. The flop-para transition of an unstrained sample is shown in (c). Figure 4 (d) gives the relation between the antiflop field H_{c1} and the flop-para field H_{c2} for differential strained samples; the error in H_{c1} is about 0.1 kOe.